Inverse Kinematics for Control of Tensegrity Soft Robots: Existence and Optimality of Solutions

Andrew P. Sabelhaus[1], Adrian K. Agogino[2]

***Abstract*— Tension-network ('tensegrity') robots encounter many control challenges as articulated soft robots, due to the structures' high-dimensional nonlinear dynamics. Control approaches have been developed which use the inverse kinematics of tensegrity structures, either for open-loop control or as equilibrium inputs for closed-loop controllers. However, current formulations of the tensegrity inverse kinematics problem are limited in robotics applications: first, they can lead to higher than needed cable tensions, and second, may lack solutions when applied to robots with high node-to-cable ratios. This work provides progress in both directions. To address the first limitation, the objective function for the inverse kinematics optimization problem is modified to produce cable tensions as low or lower than before, thus reducing the load on the robots' motors. For the second, a reformulation of the static equilibrium constraint is proposed, which produces solutions independent of the number of nodes within each rigid body. Simulation results using the second reformulation on a specific tensegrity spine robot show reasonable open-loop control results, whereas the previous formulation could not produce any solution.**

I. INTRODUCTION

Tensegrity robots are a form of articulated soft robots, which consist of rigid bodies suspended in a network of cables in tension such that no two bodies contact each other [1]. Such structures are inherently soft and flexible, and many types of tensegrity robots have been designed that leverage this flexibility. These robots are able to adjust the lengths of their cables to roll [2], [3], crawl [4], [5], climb [6], and assist in quadruped locomotion as a flexible spine [7].

Control of tensegrity robots has proven challenging. Model-based control has mostly been limited to low-dimensional structures [8], [1], [9], customized applications [10], or else, machine learning is used [4], [5], [11], [12]. An alternative for simple, rapid testing is open-loop control [13], [6], [14]. Open-loop equilibrium inputs can also be used as a reference trajectory for closed-loop control [15].

This work presents two variations on the inverse kinematics problems for tensegrity structures, as a form of open-loop control. These problems solve for tensions in the robot's cables such that its rigid bodies remain in static equilibrium. For a model of the robot as $\dot{\boldsymbol{\xi}} = \boldsymbol{g}(\boldsymbol{\xi}, \boldsymbol{u})$, control inputs $\boldsymbol{u}$ are the rest lengths of the robot's cables. Specifically, if the robot has s cables, where cable k has length l_k, rest length ρ_k, spring constant κ, and damping constant c, then the scalar tension force F_k is

[1]A.P. Sabelhaus is with the Department of Mechanical Engineering, University of California Berkeley, USA, and the NASA Ames Research Center Intelligent Robotics Group, Moffett Field, CA 94035, USA apsabelhaus@berkeley.edu

[2]A.K. Agogino is with the Intelligent Systems Divison, NASA Ames Research Center, Moffet Field CA 94035 USA

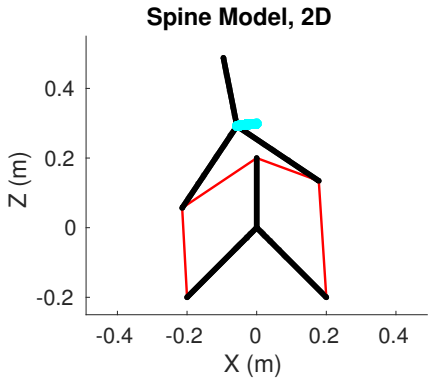

Fig. 1: Application of one inverse kinematics controller presented in this paper to an example tensegrity robot, in simulation. This two-dimensional tensegrity spine performs a counter-clockwise bend, open loop. The robot's cables, which are the control inputs to the system, are in red, and the tracked position of the moving vertebra in blue.

$$F_k = \kappa(l_k - \rho_k) - c\,\dot{l}_k \quad \in \mathbb{R}. \tag{1}$$

Then the robot's control inputs are formally defined as

$$\boldsymbol{u} = \begin{bmatrix} \rho_1 & \rho_2 & \dots & \rho_s \end{bmatrix}^\top \in \mathbb{R}^s \tag{2}$$

The inverse kinematics problem calculates F_k for each cable at a given state $\boldsymbol{\xi}$ with $\dot{l}_k = 0$, then ρ_k are calculated using eqn. (1). The following section presents the standard form of this problem as has been used in past robotics work.

II. INVERSE KINEMATICS USING THE FORCE-DENSITY METHOD

The calculation of F_k for each k becomes a statics problem, where each rigid body must be held in static equilbrium. One approach to this problem is the force-density method [6], [16], [17], [18], which solves for the minimum 2-norm of the force density in the structure subject to the static equilibrium constraint. The force-density method transforms the set of nonlinear force-balance equations into a linear system, and its solution leads to approximately minimum-force control inputs at an equilibrium point.

A. Force Density Method for Tensegrity Networks

The force density method for tensegrity systems, as networks of force-carrying structural members in tension or compression, is outlined below. Here, we present a solution for a 2D tensegrity structure (in the x,z plane), though the results are generalizable to 3D tensegrity robots.

A tensegrity structure has s members in tension (cables), r members in compression (bars, or parts of a rigid body), n nodes, in a d-dimensional space (here, $d = 2$.) The tensegrity structure is defined by three parameters. First, a connectivity matrix $\boldsymbol{C} \in \mathbb{R}^{(s+r)\times n}$ can be written that describes which nodes are connected by members, where the first s rows of $\boldsymbol{C}$ are assumed to correspond to cable members and the last r rows correspond to bar members. This matrix $\boldsymbol{C}$ is defined using a graph structure, where if member $k \in \{1,...,(s+r)\}$ connects nodes i and j, then i-th and j-th columns in $\boldsymbol{C}$ are set to 1 and -1 respectively for row k, as in

$$\boldsymbol{C}_{(k,i)} = 1, \qquad \boldsymbol{C}_{(k,j)} = -1 \tag{3}$$

All other entries in $\boldsymbol{C}$ are 0.

The second set of parameters are the locations of each node, $\{\boldsymbol{x},\boldsymbol{z}\} \in \mathbb{R}^n$, and the third is the set of external forces present at each node, $\{\boldsymbol{p}_x,\boldsymbol{p}_z\} \in \mathbb{R}^n$. In robotics applications such as [6], [15], $\{\boldsymbol{x},\boldsymbol{z}\}$ are calculated by a coordinate transformation of each member according to the robot's state vector. The external forces $\{\boldsymbol{p}_x,\boldsymbol{p}_z\}$ are calculated from the gravitational forces acting at point masses at each node as well as the reaction forces from the environment.

Given this definition of the structure, the forces in each member (both bars and cables) can be found which hold the system in static equilibrium. To do so, define the *force density* vector $\boldsymbol{q}$ as

$$\boldsymbol{q} = [\, q_1,\, q_2,\, q_3,\, \ldots\, q_{s+r}\,]^\top \in \mathbb{R}^{(s+r)} \tag{4}$$

such that if member k holds a force F_k along its length of l_k,

$$q_k = \frac{F_k}{l_k} \tag{5}$$

As seen in [6], [16], [17], [18] the force balance condition for static equilibrium of the structure can be stated as

$$\begin{aligned} \boldsymbol{C}^\top \mathrm{diag}(\boldsymbol{q})\boldsymbol{C}\boldsymbol{x} &= \boldsymbol{p}_x \\ \boldsymbol{C}^\top \mathrm{diag}(\boldsymbol{q})\boldsymbol{C}\boldsymbol{z} &= \boldsymbol{p}_z \end{aligned} \tag{6}$$

As also discussed in [6], [16], [18], eqn. (6) can be reorganized as

$$\boldsymbol{A}\boldsymbol{q} = \boldsymbol{p}, \tag{7}$$

$$\boldsymbol{A} = \begin{bmatrix} \boldsymbol{C}^\top \mathrm{diag}(\boldsymbol{C}\boldsymbol{x}) \\ \boldsymbol{C}^\top \mathrm{diag}(\boldsymbol{C}\boldsymbol{z}) \end{bmatrix} \in \mathbb{R}^{(nd)\times(s+r)} \tag{8}$$

$$\boldsymbol{p} = \begin{bmatrix} \boldsymbol{p}_x \\ \boldsymbol{p}_z \end{bmatrix} \in \mathbb{R}^{nd} \tag{9}$$

Solving for a specific $\boldsymbol{q}$ vector of force densities can be done by optimizing for the minimum total force density. This requires adding the constraint that cables can only carry tension forces. To do so, define two blocks of $\boldsymbol{q}$ as

$$\boldsymbol{q} = \begin{bmatrix} \boldsymbol{q}_s \\ \boldsymbol{q}_r \end{bmatrix} \tag{10}$$

so that $\boldsymbol{q}_s = [\, q_1,\, q_2,\, \ldots\, q_s\,]^\top \in \mathbb{R}^s$ are the cable force densities, and $\boldsymbol{q}_r$ are the rod force densities respectively.

With the constraint that each tension member has a minimum force density of $c \geq 0 \in \mathbb{R}$, since cables cannot carry compressive forces, the optimization problem becomes

$$\min_{\boldsymbol{q}} \ \boldsymbol{q}^\top \boldsymbol{q} \tag{11}$$

$$\text{s.t. } \boldsymbol{A}\boldsymbol{q} = \boldsymbol{p} \tag{12}$$

$$\boldsymbol{q}_s - \boldsymbol{1}_s c \geq 0 \tag{13}$$

The optimization problem of eqn. (11-13) is the standard form of tensegrity inverse kinematics as used in [6]. If a feasible $\boldsymbol{q}$ is found, the rest lengths ρ_k of each cable are back-calculated from eqn. (5) and (1).

B. Optimality and Existence of Solutions

Two issues arise with (11-13). First, its objective function optimizes for both the force densities in the cables as well as in the bars. However, in robotics applications where we assume the robot's rigid bodies to carry as much force as is required, this can lead to non-optimal solutions: the cables may carry more tension in favor of less stress in the bar elements, unnecessarily adding to motor load.

Second, issues arise with the existence of solutions to eqn. (7). Solutions exist only if $\boldsymbol{A}$ has a nonzero null space. Since $\boldsymbol{A}$ matrix has dimension $(nd)\times(s+r)$, this implies conditions on the number of nodes and members. When the tensegrity has many more cables and bars than nodes, such as in [6], then $(s+r)-(nd) > 0$, so if $\boldsymbol{A}$ is full rank, an infinite number of solutions exist to eqn. (7). However, this is not the case for all robots. This condition is discussed extensively in the structural engineering literature [19], [20], [9], [18].

III. REFORMULATION OF THE FORCE-DENSITY METHOD FOR ROBOTICS APPLICATIONS

Two approaches are proposed, addressing each concern. First, the objective function from eqn. (11) is modified, and solutions are proven to have cable tensions less than or equal to the original. Second, the constraint (7) is reformulated, so that solutions can exist for different tensegrity geometries.

A. Optimization for Cables Force Densities Only

As opposed to optimizing for the total force density in all members, an optimization problem can be written that only optimizes the cable force densities. Noting that

$$\boldsymbol{q}^\top \boldsymbol{q} = \boldsymbol{q}_s^\top \boldsymbol{q}_s + \boldsymbol{q}_r^\top \boldsymbol{q}_r, \tag{14}$$

a matrix can then be inserted into the objective to remove the $\boldsymbol{q}_r$ term, as in

$$\boldsymbol{H} = \begin{bmatrix} \mathbf{I}_s & \mathbf{0}_{s,r} \\ \mathbf{0}_{r,s} & \mathbf{0}_r \end{bmatrix}, \quad \boldsymbol{q}^\top \boldsymbol{H}\boldsymbol{q} = \boldsymbol{q}_s^\top \boldsymbol{q}_s, \tag{15}$$

so that the optimization problem of

$$\min_{\boldsymbol{q}} \ \boldsymbol{q}^\top \boldsymbol{H}\boldsymbol{q} \tag{16}$$

$$\text{s.t. } \boldsymbol{A}\boldsymbol{q} = \boldsymbol{p} \tag{17}$$

$$\boldsymbol{q}_s - \boldsymbol{1}_s c \geq 0 \tag{18}$$

now only contains $\boldsymbol{q}_s^\top \boldsymbol{q}_s$ as its objective.

This is an intuitive change, partially alluded to in [6], [15]. The following result formally characterizes this modification.

Proposition 1: The inverse kinematics optimization problem of (16-18), which only weights cable inputs, admits solutions with a total cable force density $\boldsymbol{q}_s^\top \boldsymbol{q}_s$ less than or equal to (11-13).

Proof:

Let the solution to (11-13) be $\boldsymbol{q}^{*1}$. Such a solution exists iff a solution exists to (16-18), since both have the same constraints. Assume $\boldsymbol{q}^{*1}$ exists, and consequently, that a solution $\boldsymbol{q}^{*2}$ exists to (16-18).

Denote $\boldsymbol{q}^o$ as any other $\boldsymbol{q}$ that satisfies the constraints of (17-18). By definition of the optimization problem, we have

$$\boldsymbol{q}^{*2\top} \boldsymbol{H} \boldsymbol{q}^{*2} \leq \boldsymbol{q}^{o\top} \boldsymbol{H} \boldsymbol{q}^{o} \tag{19}$$

Since $\boldsymbol{q}^{*1}$ also satisfies the constraints (17-18), pick $\boldsymbol{q}^o = \boldsymbol{q}^{*1}$. Then,

$$\boldsymbol{q}^{*2\top} \boldsymbol{H} \boldsymbol{q}^{*2} \leq \boldsymbol{q}^{*1\top} \boldsymbol{H} \boldsymbol{q}^{*1} \tag{20}$$

$$\implies \quad \boldsymbol{q}_s^{*2\top} \boldsymbol{q}_s^{*2} \leq \boldsymbol{q}_s^{*1\top} \boldsymbol{q}_s^{*1} \tag{21}$$

■

This result, although somewhat trivial and mathematically intuitive, is not necessarily obvious from a structural mechanics perspective.

This inequality is not strict. Counterexamples exist where the total cable force densities are equal for both problems. For example, let there be an inverse kinematics problem with only one solution to (11-13), denoted $\boldsymbol{q}^*$. Such a problem occurs, for example, when only one solution exists to $\boldsymbol{A}\boldsymbol{q} = \boldsymbol{p}$. In in this case, $\boldsymbol{q}^*$ is also the only solution to (16-18), and thus

$$\boldsymbol{q}^* = \boldsymbol{q}^{*1} = \boldsymbol{q}^{*2} \quad \implies \quad \boldsymbol{q}_s^{*2\top} \boldsymbol{q}_s^{*2} = \boldsymbol{q}_s^{*1\top} \boldsymbol{q}_s^{*1} \tag{22}$$

Therefore, under the assumption that the forces within the rigid bodies of the tensegrity robots can be neglected, the optimization problem with only cable force densities always results in solutions that are more optimal than (or equal to, in some cases) the original formulation.

B. Reformulation of the Static Equilibrium Constraint for a Rigid Body Force and Moment Balance

The node-graph formulation of the constraint matrix (7) can be adapted by instead considering a force/moment balance on the entirety of each rigid body, as opposed to each rigid body's individual nodes. The following derivation gives a form of this adaptation for one specific type of tensegrity robot (a two-dimensional, two-body system), and can be generalized in future work.

Assume there are b rigid bodies in the structure and that each rigid body has the same geometry, such that there are $\eta = \frac{n}{b}$ nodes per body. Also assume that $\boldsymbol{C}$ is written to be block-structured according to rigid body. Then, the $\boldsymbol{p}$ vector of external forces, eqn. (9), can be collapsed from the force for each node into the sum of forces for each rigid body:

$$\boldsymbol{p}_f = (\mathbf{I}_{db} \otimes \mathbf{1}_\eta^\top)\boldsymbol{p} \quad \in \mathbb{R}^{db} \tag{23}$$

Also, the lengths of each of the cable members can be calculated using the connectivity matrix, node positions, and an additional term to remove the rod coordinates, as in:

$$\boldsymbol{d}_x = \hat{\boldsymbol{H}}\boldsymbol{C}\boldsymbol{x}, \;\; \boldsymbol{d}_z = \hat{\boldsymbol{H}}\boldsymbol{C}\boldsymbol{z} \;\; \in \mathbb{R}^s, \quad \hat{\boldsymbol{H}} = \begin{bmatrix} \mathbf{I}_s & \mathbf{0}_{s,r} \end{bmatrix} \tag{24}$$

The force balance (without moments) for this two-dimensional two-body tensegrity can then be written as

$$\boldsymbol{A}_f \boldsymbol{q}_s = \boldsymbol{p}_f, \qquad \boldsymbol{A}_f = \begin{bmatrix} -\boldsymbol{d}_x \\ \boldsymbol{d}_x \\ -\boldsymbol{d}_z \\ \boldsymbol{d}_z \end{bmatrix} \in \mathbb{R}^{db \times s} \tag{25}$$

For structures with $b > 2$ rigid bodies, where sets of cables apply forces to multiple bodies, or $d = 3$ dimensions, the $\boldsymbol{A}_f$ matrix will have a more complicated block structure.

A moment balance for all rigid bodies is also required now, since the point-mass formulation has been transformed into a rigid body formulation. Denote the moment contribution from cable k around the center of mass for rigid body b as $M_{(b,k)}$, a scalar for $d = 2$. Also denote the moments due to external reaction forces (from $\boldsymbol{p}$) as M_b^e. Note that both of these quantities could be calculated automatically from $\{\boldsymbol{C}, \boldsymbol{x}, \boldsymbol{z}, \boldsymbol{p}\}$, although derivations are not provided here.

Combine the $M_{(b,k)}$ moments into row vectors for each body as $\boldsymbol{M}_b = [M_{(b,1)}, \ldots, M_{(b,s)}]$. Then, the moment balance due to all cables (for b=2) is

$$\boldsymbol{A}_m \boldsymbol{q}_s = \boldsymbol{p}_m, \quad \boldsymbol{A}_m = \begin{bmatrix} \boldsymbol{M}_1 \\ \boldsymbol{M}_2 \end{bmatrix}, \quad \boldsymbol{p}_m = \begin{bmatrix} M_1^e \\ M_2^e \end{bmatrix} \tag{26}$$

As with the force balance in eqn. (25), if $b > 2$ rigid bodies, the $\boldsymbol{A}_m$ matrix will have a more complicated block structure.

The total force and moment balance is then

$$\boldsymbol{A}_b \boldsymbol{q}_s = \boldsymbol{p}_b, \quad \boldsymbol{A}_b = \begin{bmatrix} \boldsymbol{A}_f \\ \boldsymbol{A}_m \end{bmatrix}, \quad \boldsymbol{p}_b = \begin{bmatrix} \boldsymbol{p}_f \\ \boldsymbol{p}_m \end{bmatrix} \tag{27}$$

This rigid body formulation (eqn. 23-27) can be combined with the minimum force density optimization problem (eqn. 11-13) by substituting the equality constraints, as in

$$\min_{\boldsymbol{q}_s} \; \boldsymbol{q}_s^\top \boldsymbol{q}_s \tag{28}$$

$$\text{s.t. } \boldsymbol{A}_b \boldsymbol{q}_s = \boldsymbol{p}_b \tag{29}$$

$$\boldsymbol{q}_s - \mathbf{1}_s c \geq 0 \tag{30}$$

C. Existence of Solutions to the Reformulated Problem

The matrix $\boldsymbol{A}_b \in \mathbb{R}^{(b+1)d \times s}$, whereas the original constraint from the node-graph formulation has $\boldsymbol{A} \in \mathbb{R}^{(nd) \times (s+r)}$. Since a rigid body must consist of at least two nodes, $n \geq 2b$. We assume that a tensegrity structure contains at least two bodies, and note that $2b > b+1$ for $b \geq 2$. Together, this implies $n > b+1$ for $b \geq 2$. Therefore, the reformulation always reduces the number of rows in the equality constraint matrix, since $nd > (b+1)d$ for any number of dimensions.

However, the reformulation also reduces the number of colunms of the constraint matrix, from $(s+r)$ down to just s, and therefore does not always result in a reduction in the ratio of rows to columns. Therefore, this reformulation has more favorable conditions for the existence of a solution when the tensegrity robot meets the following condition:

$$(b+1)d - nd > r \tag{31}$$

However, it is the rank of the matrices $\boldsymbol{A}$ and $\boldsymbol{A}_b$ that determine the existence of solutions, not their dimension, so this condition only provides a guideline for choosing a formulation. Either the node-graph formulation or the rigid-body reformulation may admit solutions when the other may not, suggesting that both formulations be examined for any given problem.

IV. APPLICATION TO AN EXAMPLE TENSEGRITY ROBOT

The tensegrity spine robot in Fig. 1 was controlled in simulation using the solutions to problem (28-30), which were obtained via a quadratic programming solver. For this robot, eqn. (27) has solutions. More detail about the robot's geometry and equations of motion are described in [10], [15].

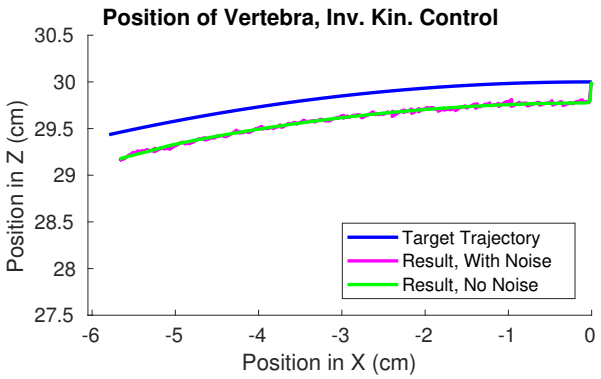

Fig. 2: Center of mass of the vertebra from Fig. 1 over 4 sec. of open-loop inverse kinematics control, in simulation. This controller produces a solution where none existed in the previous formulation. In addition, this controller can be automatically derived for any feasible structure, with the caveat that since this control is open-loop, both simulations (without noise in green and with added noise in pink) do not reject modeling error.

The simulation in Fig. 1 spans 4 sec. of motion, over 6 cm. of translation, for a 30-cm.-tall robot. The controller was operated at 10 Hz for 400 timesteps. Model error arises from a difference in assumptions in the mass distribution of the robot for the dynamics derivation. However, this result shows that control inputs exist, are reasonable, and are suitable for prototype use.

Future work will generalize this result to 3D structures with more rigid bodies, examine modeling error in more detail, provide additional analysis of the existence of solutions, and show demonstrations in hardware.

ACKNOWLEDGMENT

This work would not have been possible without the help of the many members of the Berkeley Emergent Space Tensegrities Lab and the Intelligent Robotics Group at NASA Ames Research Center. This research was supported by NASA Space Technology Research Fellowship no. NNX15AQ55H.

REFERENCES

[1] R. E. Skelton and M. C. de Oliveira, *Tensegrity systems*. Springer, 2009.

[2] A. P. Sabelhaus, J. Bruce, K. Caluwaerts, P. Manovi, R. F. Firoozi, S. Dobi, A. M. Agogino, and V. SunSpiral, "System design and locomotion of SUPERball, an untethered tensegrity robot," in *2015 IEEE International Conference on Robotics and Automation (ICRA)*. IEEE, may 2015.

[3] K. Kim, A. K. Agogino, A. Toghyan, D. Moon, L. Taneja, and A. M. Agogino, "Robust learning of tensegrity robot control for locomotion through form-finding," in *2015 IEEE/RSJ International Conference on Intelligent Robots and Systems (IROS)*. IEEE, sep 2015.

[4] C. Paul, F. Valero-Cuevas, and H. Lipson, "Design and control of tensegrity robots for locomotion," *IEEE Transactions on Robotics*, oct 2006.

[5] B. T. Mirletz, P. Bhandal, R. D. Adams, A. K. Agogino, R. D. Quinn, and V. SunSpiral, "Goal-Directed CPG-Based Control for Tensegrity Spines with Many Degrees of Freedom Traversing Irregular Terrain," *Soft Robotics*, dec 2015.

[6] J. Friesen, A. Pogue, T. Bewley, M. de Oliveira, R. Skelton, and V. Sunspiral, "DuCTT: A tensegrity robot for exploring duct systems," in *2014 IEEE International Conference on Robotics and Automation (ICRA)*. IEEE, may 2014.

[7] D. Hustig-Schultz, V. SunSpiral, and M. Teodorescu, "Morphological design for controlled tensegrity quadruped locomotion," in *2016 IEEE/RSJ International Conference on Intelligent Robots and Systems (IROS)*. Deajeon, Korea: IEEE, oct 2016.

[8] a.S. Wroldsen, M. de Oliveira, and R. Skelton, "Modelling and control of non-minimal non-linear realisations of tensegrity systems," *International Journal of Control*, mar 2009.

[9] J. M. Mirats Tur and S. H. Juan, "Tensegrity frameworks: Dynamic analysis review and open problems," *Mechanism and Machine Theory*, jan 2009.

[10] A. P. Sabelhaus, A. K. Akella, Z. A. Ahmad, and V. SunSpiral, "Model-Predictive Control of a flexible spine robot," in *2017 American Control Conference (ACC)*. IEEE, may 2017.

[11] A. Iscen, K. Caluwaerts, J. Bruce, A. Agogino, V. SunSpiral, and K. Tumer, "Learning Tensegrity Locomotion Using Open-Loop Control Signals and Coevolutionary Algorithms," *Artificial Life*, may 2015.

[12] M. Zhang, X. Geng, J. Bruce, K. Caluwaerts, M. Vespignani, V. SunSpiral, P. Abbeel, and S. Levine, "Deep reinforcement learning for tensegrity robot locomotion," in *2017 IEEE International Conference on Robotics and Automation (ICRA)*. IEEE, may 2017.

[13] C. Sultan and R. Skelton, "Deployment of tensegrity structures," *International Journal of Solids and Structures*, 2003.

[14] M. Vespignani, C. Ercolani, J. M. Friesen, and J. Bruce, "Steerable Locomotion Controller for Six-Strut Icosahedral Tensegrity robots," in *2018 IEEE/RSJ International Conference on Intelligent Robots and Systems (IROS)*, 2018.

[15] A. P. Sabelhaus, H. Zhao, E. Zhu, A. K. Agogino, and A. M. Agogino, "Model-Predictive Control with Reference Input Tracking for Tensegrity Spine Robots," in *arxiv:1806.08868*, 2018.

[16] H. J. Schek, "The force density method for form finding and computation of general networks," *Computer Methods in Applied Mechanics and Engineering*, jan 1974.

[17] A. Tibert and S. Pellegrino, "Review of Form-Finding Methods for Tensegrity Structures," *International Journal of Space Structures*, dec 2003.

[18] H. C. Tran and J. Lee, "Advanced form-finding of tensegrity structures," *Computers & Structures*, feb 2010.

[19] R. Connelly and W. Whiteley, "The Stability of Tensegrity Frameworks," *International Journal of Space Structures*, 1992.

[20] S. Pellegrino and C. Calladine, "Matrix analysis of statically and kinematically indeterminate frameworks," *International Journal of Solids and Structures*, jan 1986.